Contribution from the Department of Chemistry,
Brookhaven National Laboratory, Upton, New York 11973

4-Cyanopyridine-Bridged Binuclear and Trinuclear Complexes of Ruthenium and Iron

Nêstor E. Katz,[1] Carol Creutz,* and Norman Sutin*

Received September 15, 1987

The bis(nitrile)-bound isomer of *cis*-bis(2,2′-bipyridine)bis(4-cyanopyridine)ruthenium(II) (pK_{a2} = 2.1, pK_{a1} = 1.7 in 0.5 M aqueous NaCl) has been synthesized and used to form polynuclear species by attaching $Ru(NH_3)_5$ or $Fe(CN)_5$ moieties to the pyridine nitrogen sites. IR, UV–vis, and electrochemical data are reported for $Ru(bpy)_2(4\text{-}CNpyR)_2$, R = CH_3^+ or $Ru(NH_3)_5$, and for $Ru(bpy)_2(4\text{-}CNpy)(4\text{-}CNpyR)$, R = $Fe(CN)_5$. The nitrile stretching frequency is lower in all of the complexes (2239 cm^{-1}, R = 0; 2237 cm^{-1}, R = $Fe(CN)_5^{2-}$; 2180 cm^{-1}, R = $Ru(NH_3)_5^{2+}$) than in free 4-cyanopyridine (2243 cm^{-1}). The $Ru(bpy)_2$-centered redox potential for R = 0 is high, +1.53 V vs SSCE in CH_3CN, as are absorption and emission maxima (λ_{abs} = 404 nm in acetonitrile, λ_{em} = 555 nm in a DMF/CH_2Cl_2 glass at 77 K). The polynuclear complexes can be oxidized with Br_2 to generate valence-trapped mixed-valence complexes in which the central unit is $Ru^{II}(bpy)_2$ while the terminal M′ units ($Fe(CN)_5$ or $Ru(NH_3)_5$) are present as M′(III). Metal-to-metal charge-transfer absorption (Ru(II) to M′(III)) is observed at ~650 nm (M′ = $Ru(NH_3)_5$ in acetonitrile) and ~630 nm (M′ = $Fe(CN)_5$ in water). Both pyridine- and nitrile-bound isomers of $Ru(NH_3)_5(4\text{-}CNpy)^{2+}$ have been isolated as solids, and their properties are also reported.

Introduction

The study of charge-transfer processes in polynuclear transition-metal complexes is an established but growing field.[2-9] The electronic spectra of mixed-valence complexes may be used to infer barriers to metal-to-ligand charge-transfer processes.[3-6] In suitable systems, photoinduced charge transfer may be directly probed[7] by transient techniques. Much current interest in the transition-metal-based systems arises from the prospect of designing efficient "supramolecular" photosensitizers.[2] Thus the *cis*-$Ru(bpy)_2^{2+}$ moiety may be incorporated in a larger structure because of its desirable photophysical and photochemical properties[10-12] with other transition-metal centers being introduced to serve as electron donors or acceptors ("relays").[13] As a continuation of recent studies of 4-cyanopyridine-bridged complexes,[8] we have prepared the mononuclear, nitrile-bound *cis*-$Ru(bpy)_2(4\text{-}CNpy)_2^{2+}$ (where 4-CNpy is 4-cyanopyridine) and polynuclear species in which the 4-CNpy serves as a bridge to $Fe(CN)_5$ or $Ru(NH_3)_5$ groups through its pyridine nitrogen. Here the results of electrochemical and spectral studies of these species are described.

Experimental Section

Materials. 4-Cyanopyridine (Aldrich) was purified by recrystallization from hot 95% ethanol. HPLC grade deaerated acetonitrile was used for the spectral measurements, and it was distilled over $KMnO_4$ and P_2O_5 for the electrochemical studies. Tetrabutylammonium hexafluorophosphate (Fluka) was twice recrystallized from ethanol. Argon was deoxygenated by passing it through BASF (Cu catalyst) columns. For chromatographic separations, Sephadex LH-20 (in CH_3OH), G-25, and SP C-25 (all from Pharmacia) were used. Bromine solutions in CH_3CN were standardized by using ϵ = 183 M^{-1} cm^{-1} at 392 nm.[14] Other materials were of analytical reagent grade and were used without further purification.

Syntheses. All reactions and physical measurements were carried out in the dark by using Al foil covered containers.

***cis*-[Ru(bpy)$_2$(4-CNpy)$_2$](PF$_6$)$_2$.** A 1-g sample of *cis*-$Ru(bpy)_2Cl_2 \cdot 2H_2O$, obtained as given by Meyer et al.,[15] was added to 50 mL of water, and the suspension was heated at reflux under Ar with magnetic stirring. After 30 min, 2 g of 4-CNpy was added and heating was continued for 3 h at 60 °C and pH 2. The solution was cooled and filtered to remove unreacted solid. It was rotoevaporated to 10 mL at 60 °C, cooled, passed over a 4 × 30 cm column of Sephadex G-25 (in water) and eluted with water. To the main central fraction (~50 mL), an aqueous concentrated solution of NH_4PF_6 (2 g in 5 mL) was added dropwise. The orange precipitate was filtered, washed with ethanol and ether, and air-dried. It was twice recrystallized from acetone/ether at 0 °C and dried in a desiccator under vacuum over Drierite for 12 h. Yield: 1.45 g (81%). Anal. Calcd for $[Ru(bpy)_2(4\text{-}CNpy)_2](PF_6)_2 \cdot H_2O$: C, 41.3; H, 2.8; N, 12.0; Ru, 10.9. Found: C, 41.5; H, 2.4; N, 11.9; Ru, 10.9; Λ = 280 Ω^{-1} cm^2 mol^{-1} in acetone at 22 ± 2 °C. Comparison value for a 2:1 electrolyte: Λ = 300 Ω^{-1} cm^2 mol^{-1} for $[Ru(bpy)_3](PF_6)_2$ under the same conditions.

***cis*-[Ru(bpy)$_2$(4-CNpyCH$_3$)$_2$](PF$_6$)$_4$** was prepared in only low yield: 0.1 g of $Ru(bpy)_2CO_3$[16] was stirred under Ar for 15 min in 10 mL of 0.1 M CF_3SO_3H, then 0.5 g of $(4\text{-}CNpyCH_3)(CF_3SO_3)$ in 10 mL of 0.1 M CF_3SO_3H was added, and the solution was heated at reflux under Ar for 24 h in the dark. The solution was cooled and loaded onto a 3 × 8 cm Sephadex SP C-25 column. Mixed complexes were eluted by 0.2 and 0.3 M HCl while the desired 4+ complex (λ_{max} = 412 nm) was eluted by 0.4 M HCl. This fraction was rotoevaporated to 5 mL, mixed with NH_4PF_6 (1 g in 1 mL of water), and cooled at 0 °C for 30 min. The solid was collected on a filter, washed with ethanol and ether, and dried under vacuum. Yield: 20 mg (8%). Anal. Calcd for $[Ru(bpy)_2(4\text{-}CNpyCH_3)_2](PF_6)_4 \cdot 3H_2O$: C, 31.8; H, 2.8; N, 8.7; Ru, 7.9; PF_6, 45. Found: C, 32.5; H, 2.3; N, 8.5; Ru, 7.5; PF_6, 42.

***cis*-[Ru(bpy)$_2$(4-CNpy)$_2$Fe(CN)$_5$].** The more soluble chloride salt was prepared from 91.2 mg of *cis*-$[Ru(bpy)_2(4\text{-}CNpy)]_2(PF_6)_2 \cdot H_2O$ (0.10 mmol) by treatment with a stoichiometric amount of Ph_4AsCl in 10 mL of water. After filtration, 32.6 mg of $Na_3[Fe(CN)_5NH_3] \cdot 3H_2O$ (0.10 mmol), which was prepared and purified according to published procedures,[17,18] was added under Ar, and the mixture was stirred for 30 min. The color changed immediately from yellow to red. Then 5 mL of bromine water 0.05 M (in 0.1 M KBr) was added. After 15 min, the green precipitate was filtered, washed with water, ethanol, and ether, and stored in a desiccator under vacuum over Drierite. Yield: 45 mg (49%). Anal. Calcd for $[Ru(bpy)_2(4\text{-}CNpy)_2Fe(CN)_5] \cdot 6H_2O$: C, 48.5; H, 3.9; N, 19.9; Ru, 11.0; Fe, 6.1. Found: C, 48.8; H, 3.3; N, 19.7; Ru, 10.0; Fe, 5.5. The observed values for Ru and Fe are somewhat low, but in the correct ratio.

***cis*-[Ru(bpy)$_2$(4-CNpy)$_2$Ru$_2$(NH$_3$)$_{10}$](PF$_6$)$_6$.** Solid *cis*-$[Ru(bpy)_2(4\text{-}CN\text{-}py)_2](PF_6)_2 \cdot H_2O$ (0.12 g, 0.13 mmol) and $[Ru(NH_3)_5(H_2O)](PF_6)_2$

(1) On leave of absence from Facultad de Bioquímica, Química y Farmacia, Universidad Nacional de Tucumán, Tucumán, Argentina. Member of the "Carrera del Investigador Científico", CONICET, Argentina.
(2) Scandola, F.; Bignozzi, C. A.; Balzani, V. In *Homogeneous and Heterogeneous Photocatalysis*; Pelizzetti, E., Serpone, N., Eds.; D. Reidel: New York, 1986; pp 29–49.
(3) Hush, N. S. *Prog. Inorg. Chem.* **1967**, *8*, 391.
(4) Taube, H. *Pure Appl. Chem.* **1975**, *44*, 25.
(5) Meyer, T. J. In *Mixed Valence Compounds*; Brown, D. B., Ed.; NATO Advanced Study Institute Series 58; D. Reidel: Boston, MA, 1980.
(6) Creutz, C. *Prog. Inorg. Chem.* **1983**, *30*, 1.
(7) Creutz, C.; Kroger, P.; Matsubara, T.; Netzel, T. L.; Sutin, N. *J. Am. Chem. Soc.* **1979**, *101*, 5442. Curtis, J. C.; Bernstein, J. S.; Schmehl, R. H.; Meyer, T. J. *Chem. Phys. Lett.* **1981**, *81*, 48. Schanze, K. S.; Neyhart, G. A.; Meyer, T. J. *J. Phys. Chem.* **1983**, *90*, 2182.
(8) Cutin, E. H.; Katz, N. E. *Polyhedron* **1987**, *6*, 159.
(9) Szecsy, A. P.; Haim, A. *J. Am. Chem. Soc.* **1982**, *104*, 3063.
(10) Peterson, S. H.; Demas, J. N. *J. Am. Chem. Soc.* **1979**, *101*, 6571.
(11) Caspar, J. V.; Meyer, T. J. *Inorg. Chem.* **1983**, *22*, 2444.
(12) Pinnick, D. V.; Durham, B. *Inorg. Chem.* **1984**, *23*, 1440.
(13) (a) Bignozzi, C. A.; Roffia, S.; Scandola, F. *J. Am. Chem. Soc.* **1985**, *107*, 1644. (b) Toma, H. E.; Auburn, P. R.; Dodsworth, E. S.; Golovin, M. N.; Lever, A. B. P. *Inorg. Chem.* **1987**, *26*, 4257.
(14) Callahan, R. W.; Brown, G. M.; Meyer, T. L. *Inorg. Chem.* **1975**, *14*, 1443.
(15) Sullivan, B. P.; Salmon, D. J.; Meyer, T. J. *Inorg. Chem.* **1978**, *17*, 3334.
(16) Johnson, E. C.; Sullivan, B. P.; Salmon, D. J.; Adeyemi, S. A.; Meyer, T. J. *Inorg. Chem.* **1978**, *17*, 2211.
(17) Kenney, D. J.; Flynn, T. P.; Gallini, J. G. *J. Inorg. Nucl. Chem.* **1961**, *20*, 75.
(18) Jwo, J. J.; Haim, A. *J. Am. Chem. Soc.* **1976**, *98*, 1172.

0020-1669/88/1327-1687$01.50/0

(0.13 g, 0.26 mmol), prepared as in ref 19, were dissolved in 20 mL of deaerated acetone in a serum bottle, and the mixture was stirred under Ar for 4 h. The solution was then passed over a 3 × 20 cm Sephadex LH-20 column and eluted with CH_3OH. The main fraction was added, with stirring, to 200 mL of CH_2Cl_2. After 0.5 h, the red precipitate was filtered and washed with CH_2Cl_2 and ether. It was recrystallized from acetone/ether at 0 °C and dried under vacuum over Drierite. Yield: 0.15 g (60%). Anal. Calcd for $[Ru(bpy)_2(4\text{-}CNpy)_2Ru_2(NH_3)_{10}](PF_6)_6 \cdot 2CH_3COCH_3$: C, 23.1; H, 3.3; N, 12.7; Ru, 15.3. Found: C, 23.0; H, 2.8; N, 12.8; Ru, 15.0.

For the UV–vis measurements *cis*-$Ru(bpy)_2[(4\text{-}CNpy)Ru(NH_3)_5]_2^{7+}$ and $Ru(bpy)_2[(4\text{-}CNpy)Ru(NH_3)_5]_2^{8+}$ were prepared in situ in acetonitrile by adding stoichiometric amounts of Br_2 to $Ru(bpy)_2[(4\text{-}CNpy)Ru(NH_3)_5]_2^{6+}$. The solid 7+ ion (for IR) was isolated by evaporating to dryness a solution of the 6+ species that had been treated with 1 equiv of Br_2. A solid sample of the 8+ ion was prepared for IR by adding ether to an acetonitrile solution of the 8+ complex (generated by Br_2 oxidation of the 6+ complex) in the presence of excess tetrabutylammonium hexafluorophosphate (TBAH). The precipitate that formed was washed with ether and dried in vacuum. It was slightly contaminated with TBAH but adequate for the IR measurements.

$[Ru(NH_3)_5(4\text{-}CNpy)](PF_6)_2$. Some properties of the pyridine-bonded complex have been described,[20] but it was not isolated as a solid. A chromatographic procedure was devised to separate this ion from the nitrile-bonded isomer. A 0.3-g sample of $[Ru(NH_3)_5(OSO_2CF_3)](CF_3SO_3)_2$, obtained as in ref 21, was dissolved in 5 mL of deaerated H_2O, and Ar was bubbled through the solution for 15 min. Then 2 g of amalgamated zinc was added, and the solution was stirred for 30 min before 0.5 g of 4-CNpy dissolved in ~10 mL of deaerated H_2O was added. The solution (pH ≃4) was left for 30 min and loaded onto a Sephadex SP C-25 column (2.4 × 8 cm). The first colored (λ_{max} = 502 nm) fraction was eluted with 0.2 M HCl, rotoevaporated to ~10 mL, and then mixed with 2 g of NH_4PF_6 in 2 mL of water. The suspension was stored in the refrigerator overnight, filtered, and washed with ethanol and ether. Purification was achieved by dissolving in acetone and reprecipitating with ether. Yield: 29 mg (10%). Anal. Calcd for $[Ru(NH_3)_5(4\text{-}CNpy)](PF_6)_2 \cdot 2.5H_2O$: C, 11.5; H, 3.8; N, 15.7. Found: C, 11.5; H, 3.3; N, 15.1 (λ_{max} = 502 nm (500 nm lit.[20])). The second colored (λ_{max} = 528 nm) fraction, eluted from the column with 0.4 M HCl, contained the nitrile-bonded isomer $Ru(NH_3)_5(4\text{-}CNpyH)^{3+}$ that can be deprotonated (by addition of NaOH) to give nitrile-bound $Ru(NH_3)_5(4\text{-}CNpy)^{2+}$, both of which have previously been described.[20]

Instrumentation and Techniques. A Nicolet MX-1 FT-IR spectrophotometer was used to record IR spectra as KBr pellets. UV–visible spectra were measured at room temperature with 1-cm quartz cells by using Cary 210, Cary 17, and HP 8451A spectrophotometers. pH measurements were done with a Metrohm 632 pH meter calibrated with standard buffers. Cyclic voltammetry experiments were done with a BAS-100 electrochemical analyzer produced with a three-electrode conventional cell (Pt working and auxiliary electrodes and saturated sodium chloride calomel (SSCE) as reference electrode). Millimolar solutions of the complexes were bubbled with Ar prior to measurements at ambient temperature, 22 ± 2 °C. A Perkin-Elmer MPF-4 spectrofluorimeter was used to record the emission spectra of Ar-degassed 10^{-5} M solutions at 298.2 and 77 K (as CH_2Cl_2/DMF 1:9 glasses). Microanalyses of C, H, and N were done by Schwarzkopf Microanalytical Laboratory, while Ru and Fe were determined by using X-ray fluorescence and atomic absorption techniques.

Results

cis-$[Ru(bpy)_2(4\text{-}CNpy)_2](PF_6)_2$ was slightly soluble in water and the alcohols but was soluble in acetone, dichloromethane, acetonitrile and *N*,*N*-dimethylformamide. $Ru(bpy)_2(4\text{-}CNpy)_2Fe(CN)_5$ was only slightly soluble in water or organic solvents but was soluble in 1:1 CH_3OH/CH_3NO_2. $[Ru(bpy)_2(4\text{-}CNpy)_2Ru_2(NH_3)_{10}](PF_6)_6$ was soluble in water and organic solvents. The $Ru(bpy)_2(4\text{-}CNpy)_2^{2+}$ complex was light sensitive. Upon exposure to room light, its acetonitrile solutions gave $Ru(bpy)_2(CH_3CN)_2^{2+}$ as a final product.[22] The trinuclear $Ru(bpy)_2(4\text{-}CNpy)_2Ru_2(NH_3)_{10}^{6+}$, as well as its oxidized derivatives, was stable in room light, at least over 1 day. The acidic aqueous solutions of $Ru(bpy)_2(4\text{-}CNpy)_2^{2+}$ were stable over 2–3 h. However, alkaline solutions decomposed very quickly (in less than 1 min at pH 11), probably as a result of hydrolysis of the nitrile function.[23,24]

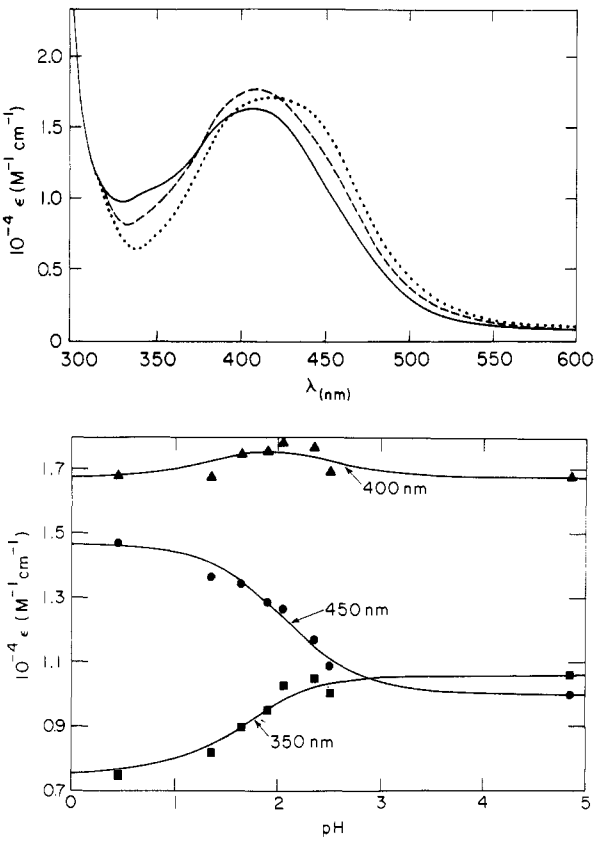

Figure 1. (a) Spectra of $Ru(bpy)_2(4\text{-}CNpy)_2^{2+}$ (pH 4.9, solid curve), $Ru(bpy)_2(4\text{-}CNpyH)(4\text{-}CNpyH)^{3+}$ (pH 1.9, dashed curve) and $Ru(bpy)_2(4\text{-}CNpyH)_2^{4+}$ (pH 0.45, dotted curve) in aqueous solution with μ = 0.5 M (NaCl). (b) Plots of molar absorptivity of $Ru(bpy)_2(4\text{-}CNpy)_2^{2+}$ at 400, 450, and 350 nm as a function of pH. Curves are calculated for pK_{a1} = 1.7 and pK_{a2} = 2.1.

An aqueous solution of $[Ru(bpy)_2(4\text{-}CNpy)_2]Br_2$ (prepared by metathesis of the PF_6^- salt) was titrated with 1 M HCl at 0.5 M ionic strength (NaCl). Initial (pH 4.9), intermediate (pH 1.87), and final (pH 0.45) spectra are presented in Figure 1a. The nitrile-bound isomer $Ru(bpy)_2L_2^{2+}$ is expected to be dibasic, i.e.

$$Ru(bpy)_2(LH)_2^{4+} \rightleftharpoons Ru(bpy)_2L(LH)^{3+} + H^+ \quad pK_{a1}$$

$$Ru(bpy)_2L(LH)^{3+} \rightleftharpoons Ru(bpy)_2L_2^{2+} + H^+ \quad pK_{a2}$$

Plots of the absorbance data at 350 and 450 nm vs pH (Figure 1b) show only a single inflection at pH ~1.9. However, the presence of the intermediate monoprotonated species is evident from the 400-nm data. At 400 nm a maximum is found at pH ~2. The data suggest that pK_{a2} and pK_{a1} are not very different and that their average value is ~2. The curves in Figure 1b are drawn for pK_{a1} = 1.7 and pK_{a2} = 2.1 and provide an adequate fit of the data.

The polynuclear Ru(II)–Fe(II) species $Ru(bpy)_2(4\text{-}CNpy)_2[Fe(CN)_5]^-$ and $Ru(bpy)_2(4\text{-}CNpy)_2[Fe(CN)_5]_2^{4-}$ were not isolated as solids. However, observations made on the solutions merit reporting. When $Ru(bpy)_2(4\text{-}CNpy)_2^{2+}$ and $Fe(CN)_5NH_3^{3-}$ were mixed in water, a red solution (λ_{max} 512, 400 nm) resulted. When the solution was chromatographed on Sephadex G-25, two bands

(19) Sutton, J. E.; Taube, H. *Inorg. Chem.* **1981**, *20*, 3125.
(20) (a) Clarke, R. E.; Ford, P. C. *Inorg. Chem.* **1970**, *9*, 495. (b) Allen, R. J.; Ford, P. C. *Inorg. Chem.* **1972**, *11*, 679.
(21) Lawrance, G. A.; Lay, P. A.; Sargeson, A. M.; Taube, H. *Inorg. Synth.* **1986**, *24*, 258.
(22) (a) Durham, B.; Walsh, J. L.; Carter, C. L.; Meyer, T. J. *Inorg. Chem.* **1980**, *19*, 860. (b) Allen, L. R.; Craft, J. P.; Durham, B.; Walsh, J. *Inorg. Chem.* **1987**, *26*, 53 and references cited therein.
(23) Breslow, R.; Fairweather, R.; Keana, J. *J. Am. Chem. Soc.* **1967**, *89*, 2135. Buckingham, D. A.; Keene, F. R.; Sargeson, A. M. *J. Am. Chem. Soc.* **1973**, *95*, 5649. Zanella, A. W.; Ford, P. C. *Inorg. Chem.* **1975**, *14*, 42.
(24) Most previous work involved trivalent metal centers.[23] Promotion of hydrolysis by a Ru(II) center has not previously been found.

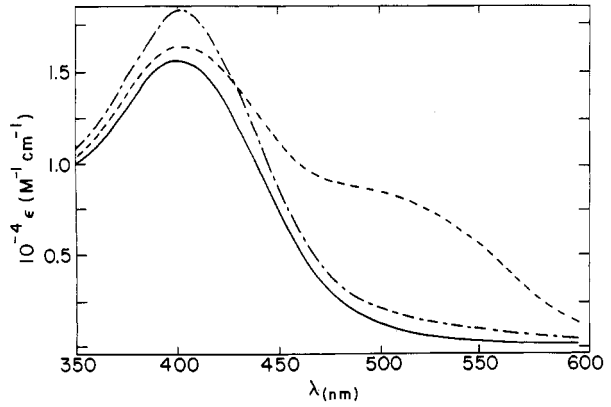

Figure 2. Spectra of $Ru(bpy)_2(4\text{-}CNpy)_2^{2+}$ (–), $Ru(bpy)_2(4\text{-}CNpy)_2Fe^{II}(CN)_5^-$ (---), and $Ru(bpy)_2(4\text{-}CNpy)_2Fe^{III}(CN)_5$ (–·) in aqueous solution (pH ~4).

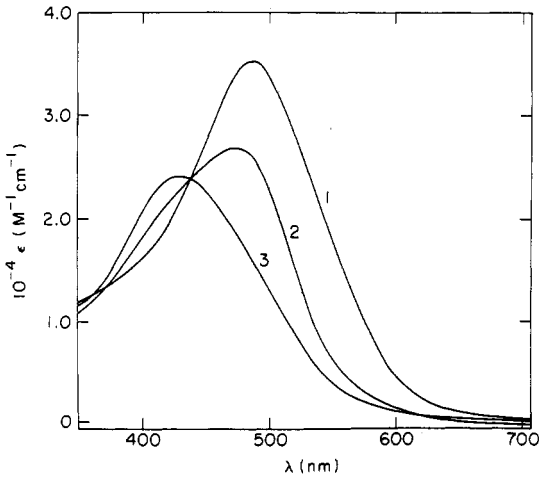

Figure 3. Visible spectrophotometric titration of $Ru(bpy)_2[(4\text{-}CNpy)Ru(NH_3)_5]_2^{6+}$ with bromine in acetonitrile at 22 ± 2 °C. $[Br_2]/[complex]$ mole ratios: solution 1, 0; solution 2, 0.5; solution 3, 1.0.

resulted, with the second band (smaller molecule) being the major one (~10 times greater than the first band). The major band is the binuclear Ru(II)–Fe(II) adduct, and the minor band, the trinuclear Ru(II)–$[Fe(II)]_2$ adduct. Both species have absorption maxima at 512 and 400 nm, but the relative intensity of the 512-nm band is 2 times greater for the trinuclear species. This new band, absent in the reactants and responsible for the color change from yellow to red, is attributed to $d\pi(Fe) \rightarrow \pi^*(4\text{-}CNpy)$ MLCT. Consistent with this assignment, the band is bleached upon oxidation of the solution with Br_2, as illustrated in Figure 2 (and regenerated by the reductant N_2H_4). In mononuclear pyridine-bonded $Fe(CN)_5(4\text{-}CNpy)^{3-}$, the MLCT band is observed at 476 nm in water.[25] Such a shift to longer wavelength is normally observed in bridged systems with Fe(II) coordinated to the pyridine nitrogen.[26,27]

The mixed-valence Ru(II)–Fe(III) binuclear species $Ru(bpy)_2(4\text{-}CNpy)_2Fe(CN)_5$, isolated as a solid after Br_2 oxidation of the reduced dimer, has absorption maxima at 410, 630, and 930 nm in methanol–nitromethane solution. However, the 930-nm band was not observed in freshly oxidized aqueous (D_2O) solutions. Thus the 930-nm band is probably due to an impurity (probably a μ-cyano species). The ca. 600-nm band was observed in freshly oxidized D_2O solutions and its half-width[3] ($\Delta\nu_{1/2}$) was $\sim 6 \times 10^3$ cm^{-1}.

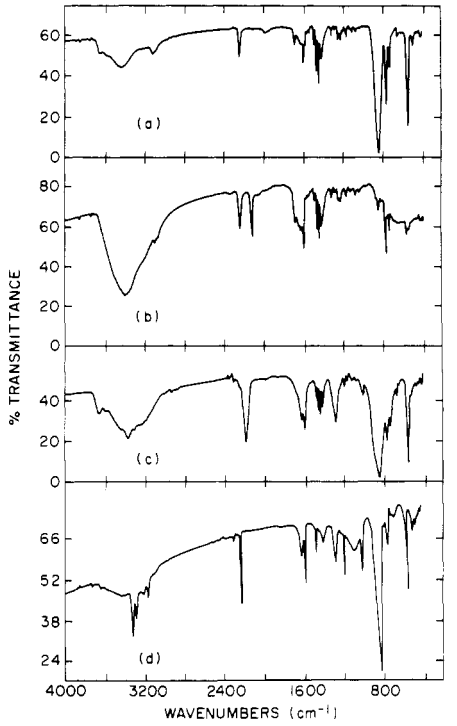

Figure 4. IR spectra obtained as KBr pellets of (a) $Ru(bpy)_2(4\text{-}CNpy)_2^{2+}$ (PF_6^- salt), (b) $Ru(bpy)_2(4\text{-}CNpy)_2Fe(CN)_5$, (c) $Ru(bpy)_2[(4\text{-}CNpy)Ru(NH_3)_5]_2^{6+}$ (PF_6^- salt), and (d) $(NH_3)_5Ru(4\text{-}CNpy)^{2+}$ (py-bonded) (PF_6^- salt).

Table I. Nitrile Stretching Frequencies in Ruthenium(II) 4-Cyanopyridine Complexes[a]

complex	ν_{CN}, cm^{-1}
NCpy	2243[b]
$Ru(bpy)_2(NCpy)_2^{2+}$	2239
$(NCpyCH_3)I$	2245
$Ru(bpy)_2(NCpyCH_3)_2^{4+}$	2254 sh, 2239
$Ru(bpy)_2(NCpy)_2(Fe(CN)_5)$	2237
$Ru(bpy)_2[(NCpy)Ru(NH_3)_5]_2^{6+}$	2180
$Ru(bpy)_2[(NCpy)Ru(NH_3)_5]_2^{7+}$	2228, 2171[c]
$Ru(bpy)_2[(NCpy)Ru(NH_3)_5]_2^{8+}$	2230
$(NH_3)_5Ru(NCpy)^{2+}$ (NC bonded)	2179[b]
$(NH_3)_5Ru(pyCN)^{2+}$ (py bonded)	2237
$(NH_3)_5Ru(NCpy)Fe(CN)_5^-$	2179[d]
$(NH_3)_5Ru(pyCN)Ru(NH_3)_5^{4+}$	2190[e]

[a] PF_6^- salt as KBr pellet unless otherwise noted. [b] Taken from ref 20. [c] Mixed Br^-, PF_6^- salt. [d] Taken from ref 8. [e] Taken from ref 42.

A redox spectrophotometric titration was performed by adding bromine to acetonitrile solutions of $Ru(bpy)_2[(4\text{-}CNpy)Ru(NH_3)_5]_5^{6+}$ ([Ru(II)Ru(II)Ru(II)]), and the spectra obtained are shown in Figure 3. The original spectrum could be recovered completely by adding Sn(II) (as $SnCl_2 \cdot 2H_2O$) to both oxidized derivatives. Addition of N_2H_4 did not completely regenerate the [Ru(II)Ru(II)Ru(II)] complex, possibly because of secondary reactions.[28] In aqueous 1 M H_2SO_4, some slow decomposition took place, but rapid titration with Ce(IV) gave spectra similar to those in Figure 3. The longest wavelength band in the trinuclear 6+ species (486 nm in acetonitrile, Figure 3) is solvent sensitive, shifting to 534 nm in *N,N*-dimethylformamide. As discussed later, the spectra of all these species contain overlapping charge-transfer bands. Since intensity in the 500-nm region is reduced upon addition of Br_2 and bleached entirely after addition of 1 mol of Br_2/mol of 6+ (Figure 3), the ~490 nm absorption is attributed to the presence of the $Ru(NH_3)_5^{2+}$ moiety. As found for the $Fe(CN)_5$ adduct, Br_2 is not a strong enough oxidant to oxidize the $Ru^{II}(bpy)_2$ unit. Thus addition of 1 mol of Br_2/mol of 6+

(25) (a) Moreno, N. G. del V.; Katz, N. E.; Olabe, J. A.; Aymonino, P. J. *Inorg. Chim. Acta* **1979**, *35*, 183. (b) García Posse, M. E.; Juri, M. A.; Aymonino, P. J.; Piro, O. E.; Negri, H. A.; Castellano, E. E. *Inorg. Chem.* **1984**, *23*, 948.
(26) Pfenning, K. J.; Lee, L.; Wohlers, H. D.; Petersen, J. D. *Inorg. Chem.* **1982**, *21*, 2477.
(27) Haim, A. *Pure Appl. Chem.* **1983**, *55*, 89.
(28) Powers, M. J.; Callahan, R. W.; Salmon, D. J.; Meyer, T. J. *Inorg. Chem.* **1976**, *15*, 894.

Table II. $E_{1/2}$ Values for Ruthenium(II) 4-Cyanopyridine Complexes vs SSCE at 22 ± 2 °C[a]

complex	process	$E_{1/2}$, V (ΔE_p, mV)
$Ru(bpy)_2(4\text{-}CNpy)_2^{2+}$	$Ru^{III/II}$	1.53 (85)
	$L^{0/-}$	−1.29, −1.41, −1.64, −1.81[b]
$Ru(bpy)_2(4\text{-}CNpyCH_3)_2^{4+}$	$Ru^{III/II}$	1.70
$Ru(bpy)_2(4\text{-}CNpy)_2Fe(CN)_5$	$Fe^{III/II}$	0.32 (65)[c]; 0.37[d]
$Fe(CN)_5(4\text{-}CNpy)^{3-}$ (pyridine bonded)	$Fe^{III/II}$	0.31 (60)[e]
$Ru(bpy)_2[(4\text{-}CNpy)Ru(NH_3)_5]_2^{6+}$	$Ru_b^{III/II}$	1.60 (85)
	$Ru_a^{III/II}$	0.67 (84) [0.37 (68)][f]
	$Ru_a^{III/II}$	0.51 (81) [0.21 (60)][f]
	$L^{0/-}$	−1.29, −1.39
	$L^{0/-}$	−1.65 (irr), −1.70 (irr)
$(NH_3)_5Ru(4\text{-}CNpy)^{2+}$ (nitrile bonded)	$Ru^{III/II}$	0.56 (61)[g]
$(NH_3)_5Ru(4\text{-}CNpyCH_3)^{3+}$	$Ru^{III/II}$	0.77
	$L^{+/0}$	−0.74[h]
$(NH_3)_5Ru(4\text{-}CNpy)^{2+}$ (pyridine bonded)	$Ru^{III/II}$	0.43 (68)
$(NH_3)_5Ru(4\text{-}CNpy)Ru(NH_3)_5^{4+}$	$Ru^{III/II}$	0.44
	$Ru^{III/II}$	0.16[i]

[a] In acetonitrile, 0.1 M in tetrabutylammonium hexafluorophosphate, unless otherwise indicated. Sweep rate = 0.2 V s^{-1}. [b] Ligand reduction; ΔE_p = 60–80 mV. [c] In water, pH 4, acetate buffer, 0.3 M KCl. A small peak with $E_{1/2}$ = 0.44 V is attributed to traces of the trinuclear $Ru^{II}[Fe^{II}]_2^{4-}$ species in the solution. [d] In 1:1 CH_3NO_2/CH_3OH. [e] In 0.5 M KCl.[41] [f] In water, 0.5 M NaCl. [g] This is in good agreement with the value reported by: Moore, K. J.; Lee, L.; Mabbott, G. A.; Petersen, J. D. *Inorg. Chem.* **1983**, *22*, 1108. [h] Reference 38. [i] In 1 M CF_3SO_3H.[42]

complex leads to oxidation of the capping $Ru(NH_3)_5^{2+}$ groups but not the central Ru:

$$Ru^{II}(bpy)_2[(4\text{-}CNpy)Ru^{II}(NH_3)_5]_2^{6+} + Br_2 \rightarrow Ru^{II}(bpy)_2[(4\text{-}CNpy)Ru^{III}(NH_3)_5]_2^{8+} + 2Br^-$$

A weak, broad ($\Delta\nu_{1/2} \sim 5.0 \times 10^3$ cm^{-1}) band was observed in the 8+ spectrum at ~650 nm in acetonitrile. Its maximum shifted to ~700 nm in nitromethane. In the spectrum of the 7+ species there was significant absorption in the near-infrared region (much greater than in the 6+ spectrum), indicating a weak band at 1000 ± 100 nm with $\epsilon \sim 30$ M^{-1} cm^{-1}.

IR spectra for the new complexes $[Ru(bpy)_2(4\text{-}CNpy)_2](PF_6)_2$, $Ru(bpy)_2(4\text{-}CNpy)_2Fe(CN)_5$, $[Ru(bpy)_2[(4\text{-}CNpy)Ru(NH_3)_5]_2](PF_6)_6$, and pyridine-bound $[Ru(NH_3)_5(4\text{-}CNpy)](PF_6)_2$ are shown in Figure 4. For comparison purposes, the nitrile stretching frequencies of these species, together with those of other 4-CNpy complexes, are summarized in Table I. As shown in Figure 4, for the monomer $Ru(bpy)_2(4\text{-}CNpy)_2^{2+}$, bands characteristic[25] of bpy vibrations (1605, 1588, 1468, 1448, 1425, 1315, 1275, 1244, 763 and 731 cm^{-1}) and of 4-CNpy vibrations (2239, 1543, 1493, 1410, 1199, 1109, 1072 and 558 cm^{-1}) are observed, and these are reproduced in $Ru(bpy)_2(4\text{-}CNpy)_2Fe(CN)_5$ and $Ru(bpy)_2[(4\text{-}CNpy)Ru(NH_3)_5]_2^{6+}$ at slightly different frequencies.

Cyclic voltammograms were recorded at 0.2 V s^{-1} and the values of $E_{1/2}$ (vs SSCE) and ΔE_p ($E_{pc} - E_{pa}$) for the different processes are shown in Table II, which also includes corresponding values for related mononuclear and dinuclear species. Unless otherwise noted, both metal- and ligand-centered redox processes are chemically reversible, although the ΔE_p values are somewhat too large for electrochemical reversibility.

UV–vis absorption maxima and molar absorptivities of the complexes are given in Table III. Since the spectra generally contain extensively overlapping absorption bands, a number of the spectra were analyzed in terms of overlapping Gaussian absorption envelopes. The results of these analyses are given in supplementary Figures S1–S4, which may be found in the supplementary material.

The complex $Ru(bpy)_2(4\text{-}CNpy)_2^{2+}$ exhibited a very weak emission at 605 nm at 25 °C in several solvents, but the excitation spectrum did not resemble the absorption spectrum. Furthermore, the intensity decreased after two recrystallizations. Thus this very weak emission is probably due to small amounts of a strongly emissive impurity, such as $Ru(bpy)_3^{2+}$, as has been found for other $Ru(bpy)_2L_2^{2+}$ systems.[29] The complex thus has a very low

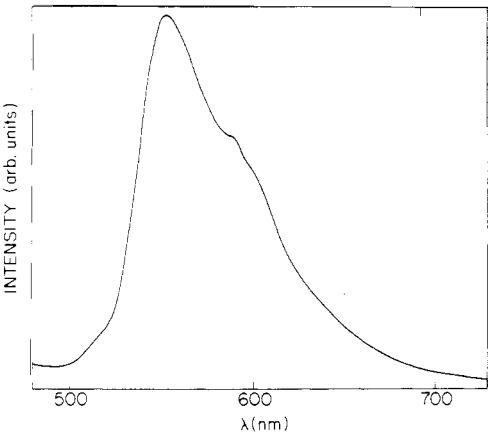

Figure 5. Corrected emission spectrum of $[Ru(bpy)_2(4\text{-}CN\text{-}py)_2](PF_6)_2$ in a DMF/CH_2Cl_2 (9:1) glass at 77 K (λ_{exc} = 410 nm).

emission quantum yield at room temperature. However, in a DMF/CH_2Cl_2 glass at 77 K there was a strong emission at 555 nm with a shoulder at 585 nm (corrected maxima) as shown in Figure 5. The excitation and absorption spectra were very similar. By analogy with related systems[11,12] the emission is attributed to radiative decay of an excited state of the $Ru(bpy)_2^{2+}$ moiety. A DMF/CH_2Cl_2 glass of $Ru(bpy)_2[(4\text{-}CNpy)Ru(NH_3)_5]_2^{6+}$ showed the same emission at 77 K, although the intensity was ~18 times weaker under identical conditions of excitation, indicating extensive quenching of the luminescence through electron- or energy-transfer processes.

Discussion

All of the species prepared here are based on the *cis*-$Ru(bpy)_2$– moiety. Although *trans*-$Ru(bpy)_2$– complexes can be prepared,[22b] our synthetic route employs thermal substitution reactions of *cis*-$Ru(bpy)_2Cl_2$ and *cis*-$Ru(bpy)_2(H_2O)_2^{2+}$, which yield *cis*-$Ru(bpy)_2L_2^{2+}$.

The 4-cyanopyridine molecule can bind a metal center through either the nitrile or the pyridine nitrogen (or, as in the polynuclear species prepared here, both nitrogens may be bound in bridged complexes). The nitrile- and pyridine-bound isomers of mononuclear complexes may be distinguished by their acid–base behavior: The nitrile-bound isomer should have one titratable site with $pK_a < 3$ (the pyridine nitrogen) for each bound 4-cyanopyridine; that of the free ligand is 1.9.[20] Thus $Ru(bpy)_2(4\text{-}CNpy)_2^{2+}$, with pK_a's of 1.7 and 2.1, contains two nitrile-bonded 4-CNpy groups. Formation of this isomer is favored by the synthetic conditions (pH 2), under which a substantial fraction of the pyridine N is protonated. In any event, the pyridine-bound isomer of $Ru(bpy)_2(4\text{-}CNpy)_2^{2+}$ was not detected in this study. By contrast, both isomers of $Ru(NH_3)_5(4\text{-}CNpy)^{2+}$ were reported by Clarke and Ford,[20] and here we have isolated both as solids. Interestingly, a ca 9:1 ratio of nitrile- to pyridine-bound isomer results even at pH ~4. This composition may reflect kinetic control ($k_{NC} > k_{py}$[20b,30]). Unfortunately, in contrast to the corresponding $Fe(CN)_5$ and $Ru(CN)_5$ complexes,[31] the relative stabilities of the two $Ru(NH_3)_5$ isomers are unknown since neither is observed to isomerize. The fact that Ru(II) complexes of 4-CNpy isomerize slowly offers controlled synthetic routes to polynuclear species of known structure. Thus, in the reactions of $Ru(bpy)_2(4\text{-}CNpy)_2^{2+}$ with $Ru(NH_3)_5OH_2^{2+}$ or $Fe(CN)_5OH_2^{3-}$, bridging to the new ($Ru(NH_3)_5$ or $Fe(CN)_5$) metal center should occur through the pyridine nitrogen. As will be seen, the spectral and electrochemical properties of the polynuclear species are consistent with this expectation.

(29) Wacholtz, W. M.; Auerbach, R. A.; Schmehl, R. H.; Ollino, M.; Cherry, W. R. *Inorg. Chem.* **1985**, *24*, 1758.
(30) Shepherd, R. E.; Taube, H. *Inorg. Chem.* **1973**, *12*, 1392.
(31) (a) Szecsy, A. P.; Miller, S. S.; Haim, A. *Inorg. Chim. Acta* **1978**, *29*, 189. (b) Almaraz, A. E.; Gentil, L. A.; Olabe, J. A., submitted for publication.

Table III. Electronic Absorption Spectra of 4-Cyanopyridine Complexes[a]

complex	λ_{max}, nm[b] ($10^{-4}\epsilon_{max}$,[c] M^{-1} cm^{-1})
$Ru(bpy)_2(4\text{-}CNpy)_2^{2+}$	404 (1.6), 366 sh (1.2), 283 (5.3), 253 (2.2), 244 (2.2), 210 sh (5.0)
$Ru(bpy)_2(4\text{-}CNpyH)_2^{4+}$	414 (1.7)
$Ru(bpy)_2(4\text{-}CNpyCH_3)_2^{4+}$	414 (1.9), 319 sh (0.82), 276 (3.9), 252 sh (2.0), 226 (3.5)
$Ru(bpy)_2(4\text{-}CNpy)_2Fe(CN)_5$[d]	630 sh (0.042), 410 (1.4)
$Ru(bpy)_2[(4\text{-}CNpy)Ru(NH_3)_5]_2^{6+}$	486 (3.4), 408 sh (1.6), 286 (5.5), 252 (4.1), 245 (4.0)
$Ru(bpy)_2[(4\text{-}CNpy)Ru(NH_3)_5]_2^{7+}$[e]	467 (2.6), 400 sh (1.8), 286 (5.6), 252 (3.9), 244 (3.8)
$Ru(bpy)_2[(4\text{-}CNpy)Ru(NH_3)_5]_2^{8+}$[e]	640 (0.07), 424 (2.3), 284 (6.0), 252 (3.7), 242 (3.7)
$Ru(NH_3)_5(4\text{-}CNpy)^{2+}$ (py bonded)	496 (1.5), 370 sh (0.092), 290 sh (0.068), 264 (0.54), 214 (0.80)
$Ru(NH_3)_5(4\text{-}CNpy)^{2+}$ (NC bonded)[f]	425 (0.54), 253 (0.89)
$Ru(NH_3)_5(4\text{-}CNpyH)^{3+}$	536 (0.87), 244 (0.81), 230 (0.67)
$Ru(NH_3)_5(4\text{-}CNpyCH_3)^{3+}$[g]	543 (1.85)
$Ru(NH_3)_5[(4\text{-}CNpy)Ru(NH_3)_5]^{5+}$[h]	493 (1.03), 935 (0.11)

[a] In acetonitrile at 22 ± 2 °C, unless otherwise indicated. [b] Error: ±2 nm. [c] Error: ±5%. [d] In methanol/nitromethane 1:1 solution. [e] Generated in acetonitrile solution by addition of stoichiometric amounts of bromine. [f] Reference 20, in water. [g] Reference 38. [h] Reference 42, in water.

The $Ru^{II}(bpy)_2$ moiety is not expected to be a strong π-donor. Thus the fact that the pK_a values of $Ru(bpy)_2(4\text{-}CNpyH)_2^{4+}$ (1.7 and 2.1) do not differ significantly from the pK_a of the free ligand (1.9[20]) and are lower than that of $Ru(NH_3)_5(4\text{-}CNpyH)^{3+}$ (2.72[20]) is not surprising. The infrared data also support a view of $Ru^{II}(bpy)_2$ as a weak π-donor, at least in the mononuclear $Ru(bpy)_2(4\text{-}CNpy)_2^{2+}$ and $Ru(bpy)_2(4\text{-}CNpyCH_3)_2^{4+}$ complexes. The nitrile stretching frequencies for the complexes studied here do occur at lower values than in the free ligand (Table I), and these shifts can be attributed to π-back-bonding from the Ru(II) of the $Ru(bpy)_2^{2+}$ moiety to the nitrile end of 4-CNpy.[20] However, the negative shift for $Ru(bpy)_2(4\text{-}CNpy)_2^{2+}$ is much smaller than that observed for the nitrile-bound $Ru(NH_3)_5(4\text{-}CNpy)^{2+}$ or other ruthenium ammine complexes (Table I), as expected because of competition between 4-CNpy and bpy for the πd-electron density in the mixed complex. In related $Ru(bpy)_2L_2^{2+}$ complexes (L = nitrile), the nitrile stretching frequency is either slightly higher than the free ligand value or is hardly changed at all,[32] so that stronger π-back-bonding for $Ru(bpy)_2(4\text{-}CNpy)_2^{2+}$ than for other bis(nitrile) complexes is inferred. The back-bonding seems to increase in the order *n*-butyronitrile (+18) < acrylonitrile (+4) < benzonitrile (0) < 4-cyanopyridine (−4), where the values in parentheses are $\Delta\nu = \nu_{CN}$(complex) − ν_{CN} (free ligand) in cm^{-1}. As might be expected, the same order seems to be found in the $Ru(NH_3)_5(nitrile)^{2+}$ series, but the shifts are much greater: acetonitrile (−15), benzonitrile (−37), and 4-CNpy (−64).[20] Significant π-acceptor ability for 4-cyanopyridine is thus inferred for $Ru(NH_3)_5^{2+}$ and, to a much smaller extent, $Ru(bpy)_2^{2+}$ centers.

For *cis*-$Ru(bpy)_2(4\text{-}CNpy)_2^{2+}$, oxidation of the metal center (eq 1) occurs with $E_{1/2}$ = 1.53 V (vs SSCE) in acetonitrile as shown in Table II. This is one of the highest potentials observed

$$Ru^{III}(bpy)_2(4\text{-}CNpy)_2^{3+} + e^- \rightarrow Ru^{II}(bpy)_2(4\text{-}CNpy)_2^{2+} \quad (1)$$

for $Ru(bpy)_2L_2^{2+}$ complexes,[32-34] indicating strong destabilization of the Ru(III) oxidation state. For bis(substituted-pyridine) derivatives, Ru(III)/Ru(II) potentials fall in the range 1.30–1.45 V,[12] while for the bis(nitrile) complexes, higher values of 1.48–1.52 V are observed.[32] Thus the present result is consistent with nitrile coordination. The four reduction processes at −1.29 to −1.81 V are attributed to ligand-centered reduction, and the assignment of these to bpy or 4-CNpy reduction is of some interest. In $Ru(bpy)_3^{2+}$, three bpy-centered (bpy/bpy^-) reductions are observed at −1.3 to −1.8 V and a second set (bpy^-/bpy^{2-}) occurs at −2.4 V and below.[35] In *cis*-$Ru(bpy)_2L_2^{2+}$ complexes in which L is a poorly reducible amine such as py or NH_3, only bpy-centered reduction is normally observed and the first occurs at −1.3 to −1.4 with the second bpy reduced by ~0.27 V negative of the first.[34] (The bpy^-/bpy^{2-} processes have not been reported, probably because they occur at very negative potentials.) The bpy/bpy^- potentials tend to shift somewhat with the Ru(III)/Ru(II) potential; as the metal center becomes a stronger oxidant, so does the ligand. Thus in $Ru(bpy)_2(4\text{-}CNpy)_2^{2+}$ the first bpy-centered reduction is expected to occur at ~−1.3 V, and the second, at ~−1.6 V (or below). In addition, 4-CNpy-centered reduction is expected. The available information[36] suggests that 4-CNpy reduction should occur at <−1.33 V in the mononuclear complex. As four reductions are observed, only two of which should be 4-CNpy centered, a reasonable assignment ascribes the first (−1.29 V) to bpy reduction.

The absorption spectrum of $Ru(bpy)_2(4\text{-}CNpy)_2^{2+}$ contains features arising from the presence of both bpy and 4-CNpy ligands. In view of their intensities, the 283–286-nm bands in these complexes must be intra-bpy π–π^* transitions,[28] while the intra-4-CNpy π–π^* transitions lie in the 250–260-nm region.[20] In addition, both Ru(II)-to-bpy and Ru(II)-to-4CNpy charge-transfer transitions are expected. On the basis of the electrochemical results for the mononuclear mixed complex, MLCT to the 4-CNpy should occur at somewhat higher energy than that to bpy. From comparisons with other compounds,[33] the Ru(II)-to-bpy MLCT band maximum should lie at ~420 nm: for $Ru(bpy)_2L_2^{2+}$, L = acrylonitrile ($E_{1/2}$ = +1.53 V), λ_{max} = 416 nm,[32] and for L = methyldiphenylphosphine ($E_{1/2}$ = +1.52 V), λ_{max} = 429 nm.[12] The observed λ_{max} = 404 nm is thus anomalous. The absorption band (see Figure 1) also lacks its characteristic shoulder at ~1300 cm^{-1} higher in frequency. These considerations suggest that the Ru(II)-to-bpy and Ru(II)-to-4-CNpy MLCT absorptions overlap to such an extent that λ_{max} is artificially shifted from ~420 to 404 nm. Thus Ru(II)-to-bpy MLCT at ~420 nm and Ru(II)-to-4-CNpy MLCT <400 nm are proposed as "true maxima". Indeed deconvolution of the 350–500-nm region of the spectrum into Gaussians (see Figure S1) yields "λ_{max}" = 426 and 360 nm.[37]

The spectral shifts that occur when $Ru(bpy)_2(4\text{-}CNpy)_2^{2+}$ is doubly protonated (Figure 1, Table III) or "methylated" are noteworthy. The most intense absorption shifts from 404 to 414 nm in $Ru(bpy)_2(4\text{-}CNpyH)_2^{4+}$ and $Ru(bpy)_2(4\text{-}CNpyCH_3)_2^{4+}$. In the latter complex, the Ru(III)/Ru(II) potential is very high, +1.70 V vs SSCE in acetonitrile. Thus the Ru(II)-to-bpy MLCT transition might be expected at shorter wavelengths than in $Ru(bpy)_2(4\text{-}CNpy)_2^{2+}$. The 414-nm bands in both the $(4\text{-}CNpyH^+)_2$ and $(4\text{-}CNpyCH_3^+)_2$ complexes are therefore most likely dominated by Ru(II)-to-$4\text{-}CNpyH^+$ (Ru(II)-to-$4\text{-}CNpyCH_3^+$) MLCT. The relatively high reduction potential of $4\text{-}CNpyCH_3^+$ (−0.7 V vs SSCE in acetonitrile[38]) is consistent with this conclusion. As above, the Ru(II)-to-bpy and Ru(II)-to-4-CNpy MLCT transitions probably overlap so as to distort the observed spectrum. A deconvolution of the absorption envelope (Figure S2) yields "λ_{max}"

(32) Keene, F. R.; Salmon, D. J.; Meyer, T. J. *J. Am. Chem. Soc.* **1976**, *98*, 1884.
(33) Dodsworth, E. S.; Lever, A. B. P. *Chem. Phys. Lett.* **1986**, *124*, 152.
(34) (a) Matsumura-Inoue, T.; Ikemoto, I.; Umezawa, Y. *J. Electroanal. Chem. Interfacial Electrochem.* **1986**, *209*, 135. (b) Sullivan, B. P.; Conrad, D.; Meyer, T. J. *Inorg. Chem.* **1985**, *24*, 3640.
(35) Tokel-Takvoryan, N. E.; Hemingway, R. E.; Bard, A. J. *J. Am. Chem. Soc.* **1973**, *95*, 6582.
(36) Kaim, W. *Inorg. Chem.* **1984**, *23*, 504.
(37) The visible spectra of other bis(nitrile) complexes of this family (e.g., benzonitrile)[32] appear to be similarly "anomalous".
(38) Curtis, J. C.; Sullivan, B. P.; Meyer, T. J. *Inorg. Chem.* **1983**, *22*, 224.

= 430 and 403 nm for MLCT to 4-CNpyH/CH_3^+ and to bpy, respectively. Thus the lowest MLCT absorption bands are different for $Ru(bpy)_2(4\text{-}CNpy)_2^{2+}$ and its conjugate acid—being Ru(II)-to-bpy in the former and Ru(II)-to-4-CNpyH$^+$ in the latter.

The high photosensitivity of $Ru(bpy)_2(4\text{-}CNpy)_2^{2+}$ is in line with the relatively high energy of the Ru(II)-to-bpy MLCT state.[12] While the latter is the lowest MLCT state of the complex, there are ligand-field (LF) states in close proximity and these are probably responsible for the photosubstitution behavior. Rapid population of the LF states could also account for the fact that no emission is detectable at ambient temperature in fluid solution. The emission observable at low temperature (Figure 5) resembles that of $Ru(bpy)_3^{2+}$ and $Ru(bpy)_2L_2^{2+}$ complexes,[12] consistent with its assignment to the decay of the Ru(II)-to-bpy MLCT excited state. In position (λ_{max} = 555 nm) it is similar to that of $Ru(bpy)_2[P(C_6H_5)_2(CH_3)]_2^{2+}$ for which λ_{max} = 547 nm, and $E_{1/2}$ for the Ru(III)/Ru(II) couple is +1.52 V vs SSCE in acetonitrile.[12]

Polynuclear Species. Both $(CN)_5Fe(II)$ and $(NH_3)_5Ru(II)$ moieties bind to $Ru(bpy)_2(4\text{-}CNpy)_2^{2+}$ to give new polynuclear complexes containing pyridine-bound $Fe(CN)_5$ and $Ru(NH_3)_5$. In $Ru^{II}(bpy)_2(4\text{-}CNpy)_2Fe^{III}(CN)_5$, the addition of a pentacyanoferrate(III) group slightly changes the nitrile stretching frequency; for $Ru^{II}(bpy)_2[(4\text{-}CNpy)Ru^{II}(NH_3)_5]_2^{6+}$, there is a dramatic shift, $\Delta\nu$ = −63 cm^{-1}, which suggests extensive π-back-bonding from the three Ru(II) centers into the 4-CNpy π^* orbitals. As shown in Figure 4, the cyanide stretching band for $Ru^{II}(bpy)_2(4\text{-}CNpy)_2Fe^{III}(CN)_5$ appears at 2115 cm^{-1}, clearly indicating oxidation state III for Fe in $Fe(CN)_5$.[39] In $Ru(bpy)_2[(4\text{-}CNpy)Ru(NH_3)_5]_2^{6+}$, bands at 3300 cm^{-1}, assigned to the N–H stretching frequency, ν_{NH}, and at 1290 cm^{-1}, assigned to the ammonia symmetric deformation, $\delta_s(NH_3)$, indicate oxidation state II for Ru in both $Ru(NH_3)_5$ units.[40] The observation of two nitrile stretching bands (and two ammonia deformation bands, 1312 and 1291 cm^{-1}) in the 7+ trinuclear species indicates the presence of distinct $Ru(NH_3)_5^{2+}$- and $Ru(NH_3)_5^{3+}$- sites. By analogy with the 6+ and 8+ spectra, the 2171-cm^{-1} band is assigned to the $Ru(NH_3)_5^{2+}$ site and the 2228-cm^{-1} band, to the $Ru(NH_3)_5^{3+}$ site.

For $Ru(bpy)_2[(4\text{-}CNpy)Ru(NH_3)_5]_2^{6+}$, oxidation of the central $Ru(bpy)_2$ moiety occurs at even higher potential than in the mononuclear complex (eq 1), as shown in Table II. In addition, the terminal $Ru(NH_3)_5^{2+}$ groups are oxidized in the 0–1 V range:

$$[Ru(III)Ru(II)Ru(III)]^{8+} + e^- \rightarrow [Ru(II)Ru(II)Ru(III)]^{7+} \quad (2)$$

$$[Ru(II)Ru(II)Ru(III)]^{7+} + e^- \rightarrow [Ru(II)Ru(II)Ru(II)]^{6+} \quad (3)$$

The difference between the potentials for eq 2 and 3 in acetonitrile and also in water is ~0.16 V. The analogues of eq 2 and 3 for the iron derivatives occur with a difference of ~0.1 V, and the first potential is very close to the value reported for pyridine-bonded $Fe(CN)_5(4\text{-}CNpy)^{3-}$.[41] From the difference ($\Delta E°$) in reduction potentials for eq 2 and 3, the equilibrium constant for comproportionation

$$[8+] + [6+] \rightleftharpoons 2[7+] \quad K_{com} \quad (4)$$

is ~500. This $\Delta E°$ for chemically equivalent $Ru(NH_3)_5$ sites is comparable to that found for some binuclear systems[42] but considerably larger than those observed for related trinuclear $Ru(bpy)_2[LRu(NH_3)_5]_2^{6+,7+,8+}$ complexes (L = pyrazine, 4,4′-bipyridine, etc.) for which a single peak is observed in cyclic voltammetry ($\Delta E° \leq 0.06$ V).[28] As noted above, the infrared spectrum of the 7+ trinuclear species indicates that both $Ru(NH_3)_5^{2+}$ and $Ru(NH_3)_5^{3+}$ sites are present in 7+; thus 7+ is a class II mixed-valence ion. The large $\Delta E°$ (or K_{com}) value for a class II species is noteworthy, especially in view of the rather large separation between the two pentaammineruthenium sites.[3,6] In the analogous cyano-bridged species, $\Delta E°$ is only ~70 mV.[13a] The relatively high stability of the 7+ mixed-valence state may result from extended π-bonding (4-CNpy-to-$Ru(III)_a$) and π-back-bonding ($Ru(II)_a$-to-4-CNpy), mediated by the interaction of the πd orbitals of the central $Ru(II)_b$ with the cis nitrile groups. Such extended π-interaction is possible in the other *cis*-$Ru(bpy)_2[LRu(NH_3)_5]_2^{7+}$ complexes (L = pz, 4,4′-bpy, etc.), as well. It may be that the small $\Delta E°$ and K_{com} values for those complexes[28] result from poor orientations of the L groups: steric repulsions may force the cis pyridine groups to twist into an orientation that "shuts off" π-interaction through the central ruthenium. Structural studies of *cis*-$Ru(bpy)_2(py)_2^{2+}$ or related complexes might help to clarify the origin of this striking difference.

The binding of low-spin d^6 $(CN)_5Fe(II)$ or $(NH_3)_5Ru(II)$ to $Ru(bpy)_2(4\text{-}CNpy)_2^{2+}$ generates the

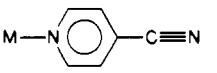

chromophore in the polynuclear species. In the mononuclear M–pyCN complexes, M-to-4-CNpy charge transfer is observed at 476 nm ($Fe(CN)_5^{3-}$)[25a] and 496 nm ($Ru(NH_3)_5^{2+}$).[20] In $Ru^{II}(bpy)_2(4\text{-}CNpy)_2Fe^{II}(CN)_5^-$ and $Ru^{II}(bpy)_2[(4\text{-}CNpy)Fe^{II}(CN)_5]_2^{4-}$ (see Figure 2) the lowest energy band (512 nm) is attributed to this transition, as is the 486-nm feature in $Ru(bpy)_2[4\text{-}CNpyRu(NH_3)_5]_2^{6+}$. The latter assignment is supported by the solvent dependence[38] of the band in the 6+ species and the molar absorptivity of the band, which is nearly twice that observed for pyridine-bonded $Ru(NH_3)_5(4\text{-}CNpy)^{2+}$ (Table III).

In polynuclear species such as $Ru(bpy)_2[(4\text{-}CNpy)Ru(NH_3)_5]_2^{6+}$ $[Ru(II)_aRu(II)_bRu(II)_b]$, several MLCT bands are possible because there are two different metal-donor sites ($Ru(II)_a$ and $Ru(II)_b$) and at least two different ligand-acceptor sites. In addition to the $Ru(II)_a$-to-4-CNpy MLCT transition discussed above, there are $Ru(II)_b$-to-bpy and $Ru(II)_b$-to-4-CNpy transitions (as discussed earlier for the mononuclear species) and a $Ru(II)_a$-to-bpy transition. The analogue of the latter has been reported for cyano-bridged species,[13] but such a band (estimated to lie at ~600 nm in acetonitrile) was not seen for the 4-CNpy-bridged species, probably because of its low intensity. The two lower energy MLCT transitions thus involve the better electron donor $Ru(NH_3)_5^{2+}$. The higher MLCT transitions involving $Ru(II)_b$ as donor are not well resolved. However, on the basis of the cyclic voltammetry (Table II) and the emission spectrum, the MLCT states arising from excitation of $Ru(II)_b$ appear to be similar in disposition to those in the parent complex $Ru(bpy)_2(4\text{-}CNpy)_2^{2+}$. The extensive quenching of emission from $Ru(bpy)_2[(4\text{-}CNpy)Ru(NH_3)_5]_2^{6+}$ when compared to the parent mononuclear complex is reasonably ascribed to enhanced nonradiative decay of the Ru(II)-to-bpy MLCT state via the lower energy Ru_a-centered MLCT states (see Table IV).

When only MLCT transitions are considered, the simplest situation obtains for the 8+ trinuclear species $[Ru(III)_aRu(II)_bRu(III)_a]$. Since both capping ($Ru_a$) centers are oxidized, there are no low-energy Ru_a MLCT transitions, and the situation is analogous to that for $Ru(bpy)_2(4\text{-}CNpy)_2^{2+}$ or $Ru(bpy)_2(4\text{-}CNpyCH_3)_2^{4+}$. The absorption spectrum and electrochemical data indicate that $[Ru(III)_aRu(II)_bRu(III)_a]$ most closely resembles $Ru(bpy)_2(4\text{-}CNpyCH_3)_2^{4+}$ or $Ru(bpy)_2(4\text{-}CNpyH)_2^{4+}$: the lowest energy absorption feature is at 424 nm, at lower energy than in the parent complex (404 nm), but the redox potential of the central Ru is higher (+1.60 vs +1.53 V) than in the parent. Thus the 424-nm feature must be dominated by $Ru(II)_b$-to-4-CNpy charge transfer. Again the $Ru(II)_b$-to-bpy MLCT transition is not well-resolved, but it is estimated to lie at ~395 nm on the basis of the $Ru(III)_b/Ru(II)_b$ reduction potential. In addition to ligand-centered states, there are metal-to-metal (MMCT) charge-transfer states (discussed later) and ligand-to-metal charge-transfer (LMCT) excited states. The latter arise from the transfer of a

(39) Della Vědova, C. O.; Alonso, S. del V.; Roncaglia, D. I.; Aymonino, P. J. *Inorg. Chim. Acta* **1983**, *73*, 221.
(40) Clarke, R. E.; Ford, P. C. *Inorg. Chem.* **1970**, *9*, 227.
(41) Brisset, J.-L.; Biquard, M. *Inorg. Chim. Acta* **1981**, *53*, L125.
(42) Richardson, D. E.; Taube, H. *J. Am. Chem. Soc.* **1983**, *105*, 40.

Table IV. Proposed Charge-Transfer Transition Energies[a]

eV	Ru(cpy)2	Ru(cpyH)2	8+	7+	6+
3.5	MLCT cpy		[LMCT cpy,a]	[LMCT cpy,a] MLCT b,cpy	MLCT b,cpy
		MLCT bpy	MLCT b,bpy		
3.0	MLCT bpy	MLCT cpy	MLCT b,cpy	MLCT b,bpy MLCT b,cpy	MLCT b,bpy
				MLCT a,cpy	
2.5			[LMCT bpy,a]	[LMCT bpy,a]	MLCT a,cpy
				[MLCT a,bpy]	
2.0			MMCT b,a	MMCT b,a	[MLCT a,bpy]
1.5					
				MMCT a,a	
1.0					
0.5					
0.0					

[a] Abbreviations: cpy, 4-cyanopyridine; bpy, 2,2′-bipyridine; "b" and "a" denote $Ru(bpy)_2$ and $Ru(NH_3)_5$ metal sites. The complexes considered are *cis*-$Ru(bpy)_2(4\text{-}CNpy)_2^{2+}$, *cis*-$Ru(bpy)_2(4\text{-}CNpyH)_2^{4+}$, *cis*-$Ru^{II}(bpy)_2[(4\text{-}CNpy)Ru^{III}(NH_3)_5]_2^{8+}$, *cis*-$Ru^{II}(bpy)_2[(4\text{-}CNpy)\text{-}Ru(NH_3)_5]_2^{7+}$, and *cis*-$Ru^{II}(bpy)_2[(4\text{-}CNpy)Ru^{II}(NH_3)_5]_2^{6+}$.

ligand-centered π electron to a $Ru(III)_a$ center to yield $Ru(II)_a(bpy^+)$ or $Ru(II)_a(4\text{-}CNpy^+)$. From the observation that $Ru(bpy)_3^{3+}$ exhibits LMCT absorption at 675 nm and the fact that $Ru(III)_a$ in the 8+ species is ~0.6 V less oxidizing than $Ru(bpy)_3^{3+}$, $\lambda_{max} \sim 500$ nm is obtained. This transition is not expected to be intense. Ligand-to-metal charge transfer (LMCT) from 4-CNpy to $Ru(III)_a$ should be more intense, but probably lies at higher energy. These assignments are also included in Table IV.

The spectrum of the 7+ trinuclear species $[Ru(II)_aRu\text{-}(II)_bRu(III)_a]$ may be considered as a sum of 6+ and 8+ spectra. Both MLCT and LMCT features should be present, but shifted somewhat from their positions in the 6+ and 8+ species because of shifts in the donor/acceptor ability of the sites. For example, $Ru(II)_a$ in the 7+ species is a poorer reductant than in the 6+ species so that $Ru(II)_a$-to-4-CNpy (and to bpy) charge transfer should be shifted to slightly higher energy. In accord with this expectation, the principal visible absorption feature, $Ru(II)_a$-to-4-CNpy MLCT, shifts from 486 nm in the 6+ species to 467 nm in the 7+ species. Analogous arguments have been used to estimate the relative positions of the other MLCT states and the LMCT and MMCT states. These estimates are summarized in Table IV.

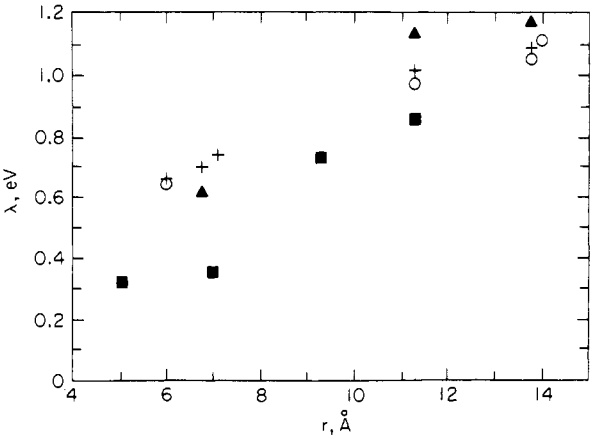

Figure 6. Plot of λ for MMCT transitions vs metal-to-metal distance for binuclear and trinuclear ruthenium species: (+) $[Ru(bpy)_2Cl]_2L^{3+}$ in acetonitrile; (○) $[Ru(NH_3)_5]_2L^{5+}$ in water; (▲) $[Ru(NH_3)_5]L[Ru\text{-}(bpy)_2Cl]^{4+}$ in acetonitrile; (■) $Ru(bpy)_2[LRu(NH_3)_5]_2^{8+}$ in acetonitrile. The λ values were obtained from eq 6. The ligands L are as follows: 5 Å, CN^-; 6 Å, pyrimidine; 6.8 Å, pyrazine; 7.1 Å, $(PPh_2)_2CH_2$; 9.3 Å, 4-CNpy; 11.3 Å, 4,4′-bpy; 13.8 Å, 4,4′-bipyridylethylene; 14 Å, 4,4′-bipyridylacetylene.

The ~650-nm bands observed for $Ru^{II}(bpy)_2(4\text{-}CNpy)_2Fe^{III}(CN)_5$ and $Ru^{II}(bpy)_2[4\text{-}CNpyRu^{III}(NH_3)_5]_2^{8+}$ (Figure S3) are attributed to MMCT transitions (eq 5a and 5b, respectively). In the $[Ru(II)_aRu(II)_bRu(III)_a]$ derivative the band

$$[Ru(II)_bFe(III)] \xrightarrow{h\nu = E_{op}} [Ru(III)_bFe(II)]^* \quad (5a)$$

$$[Ru(III)_aRu(II)_bRu(III)_a] \xrightarrow{h\nu = E_{op}} [Ru(III)_aRu(III)_bRu(II)_a]^* \quad (5b)$$

is probably obscured by the intense MLCT ($Ru(II)_a$-to-4-CNpy) band at 467 nm. In addition, there is evidence for a weak $Ru(II)_a$-to-$Ru(III)_a$ MMCT band in the near-IR region (Figure S4). MMCT band parameters from the present work and related studies are collected in Table V. The MMCT band energy E_{op} (eq 6) is comprised[3] of $\Delta E°$, the equilibrium free-energy difference[43] between the two sites, λ, which arises from inner- and

$$E_{op} = \Delta E° + \lambda + \Delta E_{ex} \quad (6)$$

Table V. Metal-to-Metal Charge-Transfer Band Parameters for Valence-Trapped Mixed-Valence Complexes at Room Temperature

complex	solvent[a]	λ_{max}, nm	ε, M^{-1} cm^{-1}	$\Delta\nu_{1/2}$, cm^{-1}	r, Å	$\Delta E°$, eV
$Ru(bpy)_2[4\text{-}CNpyRu(NH_3)_5]_2^{n+}$						
n = 8 (b,a)	CH_3NO_2	700			9.3	
n = 8 (b,a)	CH_3CN	[645]	700	[5000]	9.3	0.93
n = 7 (b,a)	CH_3CN	[625]	400			
n = 7 (a,a)	CH_3CN	[1090]	20		18.6 (13.2)[e]	0
$Ru(bpy)_2(4\text{-}CNpy)_2Fe(CN)_5$	D_2O	630	420	~6000	9.3	~0.9
$[Ru(NH_3)_5]_2(4\text{-}CNpy)^{5+}$	D_2O	935[b]	1100	5170	9.3	0.28
$Ru(bpy)_2[CNRu(NH_3)_5]_2^{n+}$						
n = 6 (b,a)	H_2O	658[c]	5700	4400	5	1.3
n = 6 (b,a)	DMF	613[c]			5	
n = 5 (a,a)	H_2O	1050[c]	400		10 (7)[e]	0
$Ru(bpy)_2[LRu(NH_3)_5]_2^{8+}$						
L = pz (b,a)	CH_3CN	730[d]	900	4100	7	1.09
L = pz (b,a)	NB	795[d]	1060		7	
L = 4,4′-bpy (b,a)	CH_3CN	605[d]			11.3	0.94
L = 4,4′-bpy (b,a)	NB	650[d]				

[a] Key: DMF, *N*,*N*-dimethylformamide; NB, nitrobenzene, "b,a" and "a,a" denote $Ru^{II}(bpy)_2$-to-$Ru(NH_3)_5^{3+}$ and $Ru(NH_3)_5^{2+}$-to-$Ru(NH_3)_5^{3+}$ MMCT, respectively. λ_{max} values in square brackets are obtained from simulation of the spectrum as a sum of Gaussians (see supplementary figures). [b] Reference 42. [c] Reference 13a. [d] Reference 28. [e] The value in parentheses is the shortest (through space) distance.

outer-shell configurational differences ($\lambda = \lambda_{in} + \lambda_{out}$), and ΔE_{ex}, in the event that the MMCT transition observed leads to an electronically excited state of the product. For the present systems ΔE_{ex} is taken as 0.25 eV.[44] In principle, λ may be evaluated from eq 7. However, since the observed width may be increased by

$$\lambda\ (cm^{-1}) = (\Delta\nu_{1/2})^2/2310 \qquad (7)$$

other factors (such as overlapping transitions to different electronic states), it is probably best to use eq 7 to obtain an upper limit on λ. The large $\Delta\nu_{1/2}$ values found here are, in any event, consistent with valence-trapped (class II) species. The electrochemical data for $Ru(bpy)_2(4\text{-}CNpy)_2Fe(CN)_5$ are incomplete, but, if the Ru_b redox potential is assumed to be equal to that observed for the mononuclear complex, $\Delta E° \sim 0.9$ eV is obtained. The E_{op}, $\Delta E°$, and ΔE_{ex} values and eq 6 may be used to estimate λ. For the 4-cyanopyridine-bridged 8+ complex, $\lambda = 0.74$ eV in acetonitrile is thus obtained.

The dependence of λ_{out} on the separation of the redox sites (r) is of considerble current interest. When data for trinuclear $Ru^{II}(bpy)_2[L(Ru^{III}(NH_3)_5]_2$ complexes in acetonitrile are combined (Table V), the distance range $r = 5.0$ (L = CN^-[13a]) to 11.3 Å (L = 4,4′-bpy[28]) is encompassed. The λ values obtained for these systems from eq 6 and the values in Table V are plotted against r in Figure 6. Also included in Figure 6 are values[6] for the symmetric $[Ru(bpy)_2Cl]_2L^{3+}$ in acetonitrile[45] and $[(NH_3)_5Ru]_2L^{5+}$ in water[46] and for asymmetric $[Ru(NH_3)_5]L[Ru(bpy)_2Cl]^{4+}$ in acetonitrile. As has been noted previously,[47] λ increases with r as expected from dielectric continuum treatments[44b] of λ_{out}. In addition λ is systematically smaller at a given r value for the trinuclear than for the binuclear species. This is reasonably ascribed to the relatively larger molecular (solvent-excluded) volumes of the trinuclear species.

Although the solvent dependence of λ_{out} is significant, the solvent dependence of the MMCT band in the trinuclear ruthenium species arises largely through the specific solvent dependence[48] of $\Delta E°$. The $E_{1/2}$ values of $Ru(NH_3)_5L^{3+/2+}$ couples are strongly solvent dependent[38,48] with the $Ru(NH_3)_5^{3+}$ moiety being a stronger oxidant in nitromethane than in acetonitrile. Thus $\Delta E°$ is smaller in nitromethane ($\lambda_{max} \sim 700$ nm) than in acetonitrile ($\lambda_{max} = 650$ nm). Note that the molar absorptivity for the $Ru(II)_b$-to-$Ru(III)_a$ MMCT transition in the 4-CNpy-bridged trinuclear ruthenium species is approximately twice that of the corresponding transition in the binuclear ruthenium-iron species (Table V): this is consistent with the fact that there are two acceptor sites in the trinuclear ruthenium complex, but only one in the binuclear complex. The much larger molar absorptivity for the CN-bridged trinuclear ruthenium complex (Table V) may reflect the shorter metal–metal separations and consequently stronger coupling in this system compared with that in the 4-CNpy-bridged trinuclear complex. As noted above, in the 7+ species an additional MMCT transition, arising from optical electron transfer between the two $Ru(NH_3)_5$ groups ($\Delta E° = 0$), is expected at relatively low energy. A weak transition is indeed found in this region (1000 ± 100 nm), and the band is of very low intensity ($\epsilon \sim 20\ M^{-1}\ cm^{-1}$). The low intensity is a consequence of the large separation between the sites: the through-bond metal-to-metal distance between the $Ru(NH_3)_5^{2+}$ and $Ru(NH_3)_5^{3+}$ sites is twice as great (18.6 Å) as that for the $Ru(bpy)_2^{2+}$–$Ru(NH_3)_5^{3+}$ sites ($\epsilon_{MMCT} = 700\ M^{-1}\ cm^{-1}$) while the "through-space" (13.2 Å) distance is about 40% greater. $Ru(II)_a$-to-$Ru(III)_a$ MMCT was not detected for the $Ru^{II}(bpy)_2[LRu(NH_3)_5]_2^{7+}$ (L = pyrazine, 4,4′-bpy, etc.) series.[28]

The complexes characterized in this study exhibit rich redox manifolds and correspondingly rich charge-transfer excited-state manifolds. The electrochemical studies indicate that $Ru(bpy)_2^{2+/3+}$, $Ru(NH_3)_5^{2+/3+}$ and $Fe(CN)_5^{4-/3-}$ sites may be oxidized/reduced and that the bound bpy and 4-CNpy ligands may also act as electron acceptors. The spectra of the complexes are also dominated by charge-transfer processes. The most intense transitions involve metal ($Ru(bpy)_2^{2+}$, $Ru(NH_3)_5^{2+}$, $Fe(CN)_5^{4-}$) to ligand (bpy or 4-CNpy) charge transfer, but metal-to-metal charge-transfer bands are also observed. Consistent with their larger size, the trinuclear ruthenium species feature lower solvent reorganization barriers for MMCT transitions compared to corresponding binuclear species (Figure 6). The greatly diminished (room-temperature) photosensitivity and reduced (low-temperature) emission of the trinuclear ruthenium derivatives compared to $Ru(bpy)_2(4\text{-}CNpy)_2^{2+}$ is encouraging since it indicates that the presence of Ru_a-centered CT states quenches deactivation via the Ru_b-centered LF states. Laser flash photolysis experiments[49] are now in progress in an effort to probe these energy- and charge-transfer processes.

Acknowledgment. A fellowship awarded to N.E.K. from the "Consejo Nacional de Investigaciones Cientificas y Tēcnicas de la Republica Argentina" is gratefully acknowledged. We also acknowledge helpful discussions with Dr. J. Winkler, and we wish to thank E. Norton for performing the Ru and Fe analyses. This research was carried out at Brookhaven National Laboratory under Contract DE-AC02-76CH00016 with the U.S. Department of Energy and was supported by its Division of Chemical Sciences, Office of Basic Energy Sciences.

Registry No. *cis*-$[Ru(bpy)_2(4\text{-}CNpy)_2](PF_6)_2$, 113810-73-4; *cis*-$[Ru(bpy)_2(4\text{-}CNpyCH_3)_2](PF_6)_4$, 113794-63-1; *cis*-$[Ru(bpy)_2(4\text{-}CNpy)_2Ru_2(NH_3)_{10}](PF_6)_6$, 113794-66-4; $Ru(bpy)_2[(NCpy)Ru(NH_3)_2]_2^{7+}$, 113794-76-6; $Ru(bpy)_2[(NCpy)Ru(NH_3)_5]_2^{8+}$, 113794-75-5; $(NH_3)_5Ru(pyCN)^{2+}$ (py bonded), 113794-68-6; $(NH_3)_5Ru(NCpy)^{2+}$ (NC bonded), 70982-10-4; $(NCpyCH_3)I$, 1194-04-3; *cis*-$Ru(bpy)_2Cl_2$, 19542-80-4; $Ru(bpy)_2CO_3$, 59460-48-9; $Na_3[Fe(CN)_5NH_3]$, 14099-05-9; $[Ru(NH_3)_5(H_2O)](PF_6)_2$, 34843-18-0; $[Ru(NH_3)_5(OSO_2CF_3)](CF_3SO_3)_2$, 113810-74-5; Br_2, 7726-95-6; $Ru(bpy)_2(4\text{-}CNpy)_2^{3+}$, 113794-69-7; $Ru(bpy)_2(4\text{-}CNpyCH_3)_2^{5+}$, 113794-70-0; $Ru(bpy)_2(4\text{-}CNpy)_2Fe(CN)_5^+$, 113794-71-1; $(NH_3)_5Ru(4\text{-}NCpyCH_3)^{3+}$, 79447-32-8; $Fe(CN)_5(4\text{-}NCpy)^{2-}$, 91209-54-0; $(NH_3)_5Ru(4\text{-}NCpy)^{3+}$ (NC bonded), 71015-99-1; $(NH_3)_5Ru(4\text{-}NCpyCH_3)^{4+}$, 113810-75-6; $(NH_3)_5Ru(4\text{-}NCpy)^{3+}$ (py bonded), 113794-72-2; $(NH_3)_5Ru(4\text{-}NCpy)Ru(NH_3)_5^{6+}$, 113794-73-3; $Ru(bpy)_2(4\text{-}CNpyH)^{4+}$, 113794-74-4; $Ru(NH_3)_5(4\text{-}CNpyH)^{3+}$, 70982-09-1.

Supplementary Material Available: Figures showing the fits of the absorption spectra of $Ru(bpy)_2(4\text{-}CNpy)_2^{2+}$, $Ru(bpy)_2(4\text{-}CNpyCH_3)_2^{4+}$, $Ru(bpy)_2[(4\text{-}CNpy)Ru(NH_3)_5]_2^{8+}$, and $Ru(bpy)_2[(4\text{-}CNpy)Ru(NH_3)_5]_2^{7+}$ to the sums of Gaussian profiles (6 pages). Ordering information is given on any current masthead page.

(43) Marcus, R. A.; Sutin, N. *Comments Inorg. Chem.* **1986**, *5*, 119.
(44) (a) Hupp, J. T.; Meyer, T. J. *Inorg. Chem.* **1987**, *26*, 2332. (b) Brunschwig, B. S.; Ehrenson, S.; Sutin, N. *J. Phys. Chem.* **1986**, *90*, 3657.
(45) Powers, M. J.; Salmon, D. J.; Callahan, R. W.; Meyer, T. J. *J. Am. Chem. Soc.* **1976**, *98*, 6731. Powers, M. J.; Meyer, T. J. *J. Am. Chem. Soc.* **1980**, *102*, 1289.
(46) Tom, G. M.; Creutz, C.; Taube, H. *J. Am. Chem. Soc.* **1974**, *96*, 7828. Tom, G. M. Ph.D. Thesis, Stanford University, 1975. Taube, H. *Ann. N. Y. Acad. Sci.* **1978**, *313*, 481.
(47) Callahan, R. W.; Brown, G. M.; Meyer, T. J. *J. Am. Chem. Soc.* **1974**, *96*, 7829.
(48) Chang, J. P.; Fung, E. Y.; Curtis, J. C. *Inorg. Chem.* **1986**, *25*, 4233.
(49) Winkler, J. R.; Netzel, T. L.; Creutz, C.; Sutin, N. *J. Am. Chem. Soc.* **1987**, *109*, 2381.